Two-electron spectra and the spin transition in ellipsoidal quantum dots

Dong Xu and Jia-Lin Zhu*
Department of Physics, Tsinghua University, Beijing 100084, China
(Received 25 January 2005; published 10 August 2005)

Size and shape effects on two-electron spectra and the spin transition in ellipsoidal quantum dots in magnetic fields are studied. Calculated results show that the level crossing of two electrons in quantum dots is dramatically influenced by the shape and size which can strongly change single-electron levels and Coulomb interaction energies. The spin transition is quite different between prolate and oblate quantum dots. The spectra are almost independent of the total spin as the vertical confinement is much weaker than the lateral one. The quantum behaviors of ellipsoidal quantum dots show some relations with those of vertically coupled quantum dots, and they are well explored.

DOI: 10.1103/PhysRevB.72.075326 PACS number(s): 73.21.La, 75.75.+a

I. INTRODUCTION

The progress in manufacturing nanostructures has given possibilities to wide experiments in low-dimensional physics and novel device applications. It is shown both theoretically and experimentally that nanostructures with reduced dimensions, relative to the bulk materials, have many interesting features, such as the quantum Hall effect and Coulomb blockade effect. Quantum dots (QD's) are one kind of nanostructures in which electrons are confined in all three directions, giving rise to a discrete spectrum of energy levels similar to that of atoms.[1,2]

Advances in semiconductor technology have made it possible to manufacture QD's at heterointerfaces in which the extension in the lateral plane is larger than that in the vertical direction, and thus the extension in the vertical direction could be effectively considered as zero in some cases. Much attention has been paid to theoretically investigate two-dimensional (2D) QD's in their energy levels and optical properties.[3–6] However, it has already been verified in experiments that the vertical confinement may become important in both self-organized and gate-defined quantum dots[7–10] since the shape of QD's as well as the size is one of critical parameters in determining their electronic and optical properties. Furthermore, recently it is possible to fabricate 3D colloidal QD's (Refs. 11–13), which exhibit many novel features, some of which are highly desirable in a variety of applications: i.e., linearly polarized emission,[14,15] improved optical gain performance,[16] and quite different exciton relaxation dynamics.[17]

Besides the experimental progress, many theoretical investigations have been done considering extensions in three directions to reveal the differences between 3D QD's and 2D ones. Energy levels of a single electron confined in ellipsoidal QD's and the far-infrared absorbtion spectrum have been calculated in the ellipsoidal coordinate.[18,19] It has been found that energy levels split with respect to those of spherical QD's as a result of the decrease in symmetry. Hole states in the valence band have been investigated by using $k\cdot p$ theory,[20,21] and the calculated optical transition polarization qualitatively agrees with the experimental measurements.[14,15] Other than single-particle states, the ground states of two electrons in ellipsoidal QD's have been calculated by using a variational approach.[22] Moreover, recent studies of two electrons in vertically coupled QD's for application as quantum gates show that vertical confinement is significant for the spin transition of the ground state.[23,24] Thus, the shape and size effects of the spectra of two electrons in ellipsoidal QD's and related properties are not only very important for themselves, but are also related to vertically coupled QD's. It however has not been systematically investigated. In this paper, we have calculated the energy levels of two-electron ellipsoidal QD's and paid much attention to the shape and size effects on Coulomb interaction energies and the spin transition.

In Sec. II, the computational method is presented for two electrons in ellipsoidal QD's. In Sec. III, shape and size effects on the energy levels and the spin transition of the ground state are shown and discussed, followed by a summary in Sec. IV.

II. HAMILTONIAN AND FORMULAS

For most QD's, a parabolic potential is a very good approximation to describe the confinement of electrons. Hence, the Hamiltonian of two electrons in ellipsoidal quantum dots with magnetic field along the z axis is

$$H = H_1 + H_2 + \frac{2}{r_{12}}, \tag{1}$$

where H_i $(i=1,2)$ is the single-electron Hamiltonian and $2/r_{12}$ is the Coulomb interaction:

$$H_i = -\nabla_i^2 + \frac{\gamma_{xy}^2}{4}\rho_i^2 + \frac{\gamma_z^2}{4}z_i^2 + \frac{\gamma_B^2}{16}\rho_i^2 + \frac{\gamma_B}{2}L_{z_i}. \tag{2}$$

Here the effective Rydberg Ry^* and the effective Bohr radius a^* are taken to be the energy and length units, respectively. The magnetic field γ_B is measured in the unit $\hbar\omega_c/\mathrm{Ry}^*$ with the cyclotron frequency ω_c. After taking a coordinate transformation in the xy plane, $\mathbf{R}=(\boldsymbol{\rho}_1+\boldsymbol{\rho}_2)/2, \mathbf{r}=(\boldsymbol{\rho}_1-\boldsymbol{\rho}_2)$, the Hamiltonian can be separated into three terms—center of mass H_R and relative motion H_r in the xy plane and the rest H':

$$H_R = -\frac{1}{2}\nabla_R^2 + \frac{\gamma^2}{2}R^2 + \frac{\gamma_B}{2}L_{ZR}, \tag{3}$$

$$H_r = -2\nabla_r^2 + \frac{\gamma^2}{8}r^2 + \frac{\gamma_B}{2}L_{zr}, \tag{4}$$

$$H' = -\frac{\partial^2}{\partial z_1^2} - \frac{\partial^2}{\partial z_2^2} + \frac{\gamma_z^2}{4}(z_1^2 + z_2^2) + \frac{2}{\sqrt{r^2 + (z_1 - z_2)^2}}, \tag{5}$$

where $\gamma = \sqrt{\gamma_{xy}^2 + \gamma_B^2/4}$. L_{ZR} and L_{zr} are the Z and z angular momentum operators in center-of-mass and relative-motion systems, respectively. The energy eigenvalues of H_R are given by $E_R(N,M) = \gamma(2N + 1 + |M|) + (\gamma_B/2)M$ with radial and azimuthal quantum numbers $N = 0, 1, 2, \ldots$ and $M = 0, \pm 1, \pm 2, \ldots$. The eigenfunctions of the H_R are given by

$$\Phi_{N,M}^R(\mathbf{R}) = \kappa(N,M)R^{|M|}L_N^{|M|}(\xi)e^{iM\phi}e^{-\gamma R^2/2}, \tag{6}$$

where $L_N^{|M|}(\xi)$ is the generalized Laguerre polynomials $\xi = \gamma R^2$ and $\kappa(N,M) = \gamma^{(|M|+1)/2}\sqrt{N!}/\sqrt{\pi(N+|M|)!}$. The plane polar coordinate $\mathbf{R} = (R, \phi)$ is used.

The eigenvalues of the H_r are also of a similar kind of form and given by $E_r(n,m) = \gamma(2n + 1 + |m|) + (\gamma_B/2)m$ with the corresponding radial and azimuthal quantum numbers $n = 0, 1, 2, \ldots$ and $m = 0, \pm 1, \pm 2, \ldots$. The eigenfunctions of H_r are given by

$$\Phi_{n,m}^r(\mathbf{r}) = \kappa(n,m)r^{|m|}L_n^{|m|}(\xi)e^{im\theta}e^{-\gamma r^2/8}, \tag{7}$$

where $\xi = \gamma r^2/4$ and $\kappa(n,m) = (\gamma/4)^{(|m|+1)/2}\sqrt{n!}/\sqrt{\pi(n+|m|)!}$. The plane polar coordinate $\mathbf{r} = (r, \theta)$ is also used.

The eigenfunctions of H' excluding the Coulomb interaction are given by

$$\Theta_{n_1,n_2,A}(z_1,z_2) = \kappa(n_1,n_2)e^{-\gamma_z(z_1^2+z_2^2)/4}[\Omega_{n_1}(\xi_1)\Omega_{n_2}(\xi_2) + (-1)^A\Omega_{n_2}(\xi_1)\Omega_{n_1}(\xi_2)], \tag{8}$$

where $\Omega_n(\xi)$ is the Hermite polynomials, $\xi_i = \sqrt{\gamma_z/2}z_i$ $(i = 1, 2)$, $\kappa(n_1,n_2) = \sqrt{\gamma_z}/\sqrt{(2+2\delta_{n_1,n_2})2^{n_1+n_2+1}n_1!n_2!\pi}$, and $A = 0, 1$ for symmetry and antisymmetry in the z axis, respectively. The eigenvalues of H' excluding the electron-electron interaction are given by $E_z(n_1,n_2,A) = \gamma_z(n_1 + n_2 + 1)$ with the corresponding quantum numbers $n_1, n_2 = 0, 1, 2, \ldots$ $(n_1 \leqslant n_2$ for $A = 0$ and $n_1 < n_2$ for $A = 1)$.

The two-electron wave function excluding the Coulomb interaction is $\Psi = \Phi_{N,M}^R(\mathbf{R})\Phi_{n,m}^r(\mathbf{r})\Theta_{n_1,n_2,A}(z_1,z_2)$. Since the Pauli exclusion principle requires the total wave function to be antisymmetric, we have spin singlet $(s = 0)$ state for even m with $A = 0$ or odd m with $A = 1$ or triplet $(s = 1)$ state for even m with $A = 1$ or odd m with $A = 0$. The total energy eigenvalues excluding the Coulomb interaction are given by

$$E_0(n,m,N,M,n_1,n_2,s) = E_R(N,M) + E_r(n,m) + E_z(n_1,n_2,A). \tag{9}$$

When the electron-electron interaction is included, we should calculate the energy eigenvalues of $H_\mathbf{r} + H'$. The eigenfunctions of $H_\mathbf{r} + H'$ could be expanded as follows:

$$\psi_{n,m,s}(\mathbf{r},z_1,z_2) = \sum_{i,j,k,j\leqslant k} C_{ijk}^{nm}\Phi_{i,m}^r(\mathbf{r})\Theta_{j,k,A}(z_1,z_2), \tag{10}$$

where n is the order of magnitude of eigenvalues with both fixed azimuthal quantum number m and spin s. The coefficient C_{ijk}^{nm} and corresponding eigenvalues $\epsilon(n,m,s)$ are calculated through diagonalization in which the matrix elements can be calculated analytically:

$$\langle\Phi_{i_1,m}^r\Theta_{j_1,k_1,A}|H_\mathbf{r} + H'|\Phi_{i_2,m}^r\Theta_{j_2,k_2,A}\rangle = V(i_1,i_2,m,j_1,k_1,j_2,k_2,A) + \delta_{i_1i_2,j_1j_2,k_1k_2}\epsilon_0(i_1,m,j_1,k_1), \tag{11}$$

where $\epsilon_0(i_1,m,j_1,k_1) = \gamma(2i_1 + |m| + 1) + \gamma_z(j_1 + k_1 + 1) + (\gamma_B/2)m$ and the Coulomb interaction term $V(i_1,i_2,m,j_1,k_1,j_2,k_2,A)$ can be analytically obtained (see the Appendix). Then the energy eigenvalues of H are given by

$$E(n,m,N,M,s) = E_R(N,M) + \epsilon(n,m,s). \tag{12}$$

The Coulomb energy E_C of states with $n = 0$ can be defined as

$$E_C(0,m,N,M,s) = E(0,m,N,M,s) - E_0(0,m,N,M,n_1,n_2,s), \tag{13}$$

where $n_1 = n_2 = 0$ for $A = 0$ and $n_1 = 0, n_2 = 1$ for $A = 1$.

III. RESULTS AND DISCUSSION

Before the calculated results are shown and discussed, it is useful to specify the labeling of the quantum levels of two electrons in ellipsoidal QD's. As illustrated in Eq. (12), the energy levels $E(n,m,N,M,s)$ can be labeled by five symbols. In Sec. III A, we give the energy levels in ellipsoidal QD's without the magnetic field. In Sec. III B, we investigate the spin transition of the ground state in magnetic field.

A. Shape and size effects on energy levels

First, we have performed numerical diagonalization for energy levels of two electrons in spherical QD's and compared the results with those in our previous works.[25] It is verified that the energy levels are in good agreement with previous exact ones with an accuracy of ground-state energy better than 0.03%. Then we have calculated two-electron energy levels for an ellipsoidal and a spherical QD and compared them as shown in Table I. It is easily seen that the level orders greatly change as the size and shape of QD's are varied.

In order to clearly reveal the size effect in two-electron ellipsoidal QD's, we have calculated two-electron energy levels with $\gamma_z/\gamma_{xy} = 4.0$ and γ_{xy} varying from 0.1 to 1000. For the sake of clearness, the calculated results are normalized by γ_{xy} and plotted as a function of $\gamma_{xy}^{-1/2}$ in Fig. 1. It is also easily found that both of the level order and the energy difference dramatically change as $\gamma_{xy}^{-1/2}$ varies.

For a better understanding of size effect, it is interesting to study the Coulomb interaction. The analytical form of the

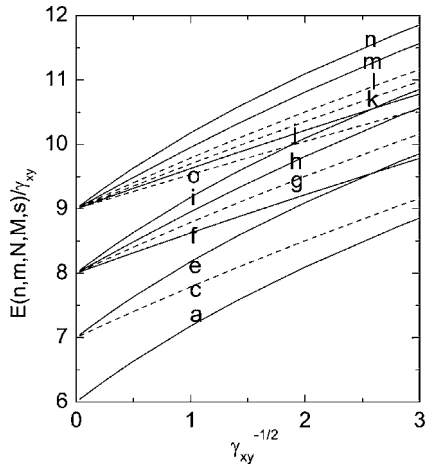

FIG. 1. Energy levels of spin-singlet (solid lines) and -triplet (dashed lines) states normalized by γ_{xy} as a function of $\gamma_{xy}^{-1/2}$ for ellipsoidal QD's with $\gamma_z/\gamma_{xy}=4$.

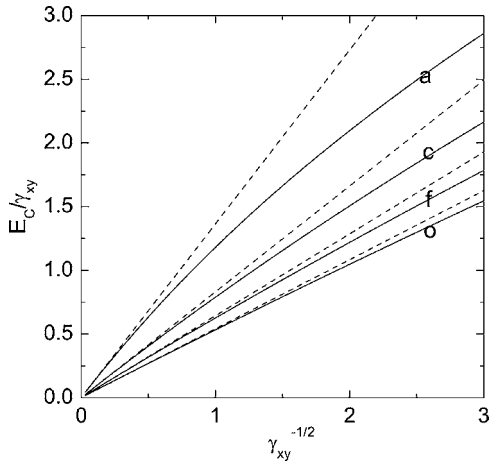

FIG. 2. Coulomb energies of ellipsoidal QD's with $\gamma_z/\gamma_{xy}=4$ defined by Eq. (13) and obtained by the exact diagonalization (solid lines) and the perturbation calculation (dashed lines) as a function of $\gamma_{xy}^{-1/2}$.

Coulomb energy E_C defined by Eq. (13) with $A=0$ is given by using perturbation theory:

$$E_C(0,m,N,M,s) = \left\langle \Phi_{0,m}^r \Theta_{0,0,0} \left| \frac{2}{\sqrt{r^2+(z_1-z_2)^2}} \right| \Phi_{0,m}^r \Theta_{0,0,0} \right\rangle = \frac{\Gamma(|m|+1)\sqrt{\lambda}\sqrt{\gamma}}{\Gamma\left(|m|+\frac{3}{2}\right)} F\left(\frac{1}{2},|m|+1;|m|+\frac{3}{2};1-\lambda\right), \tag{14}$$

where $F(\frac{1}{2},|m|+1;|m|+\frac{3}{2};1-\lambda)$ is a hypergeometric function and $\lambda=\gamma_z/\gamma$ with $\gamma=\gamma_{xy}$ for no magnetic field. The deduction refers to the Appendix. In Fig. 2, we give the E_C obtained from Eq. (14) as a function of $\gamma_{xy}^{-1/2}$ with $\lambda=4.0$ and compare them with the numerically calculated E_C defined in Eq. (13). The perturbation results are in good agreement with the numerical results if $\gamma_{xy}^{-1/2} \ll 1$ since E_C/γ_{xy} is small and E_C could be effectively considered as a perturbation. If $\gamma_{xy}^{-1/2} > 1$, Coulomb energies are comparable with or even greater than γ_{xy} and the perturbation theory becomes ineffective. As a result, both the level order and the energy difference are strongly influenced by Coulomb energies if $\gamma_{xy}^{-1/2} > 1$ as illustrated in Fig. 1.

In Figs. 3(a) and 3(b), we give the two-electron energy levels of prolate and oblate QD's, respectively, as a function of $\gamma_z^{-1/2}$ with $\gamma_{xy}=1.0$. In Fig. 3(a), the shape of QD's varies from the sphere to the prolate ellipsoid and the splitting of degeneracy in energy levels could be found due to the decrease in symmetry. As $\gamma_z^{-1/2}$ becomes greater than $\gamma_{xy}^{-1/2}$, miniband energy structures appear and their edges depend on the quantum numbers m, N, and M. It is seen that the energy difference between states a and c notated in Table I becomes larger in prolate QD's and approaches to γ_{xy}. As $\gamma_z^{-1/2}$ increases, the spin-singlet state a is always the lowest state. Meanwhile, both the energy difference between the triplet state b and the singlet state a and its ratio to γ_z dramatically decrease, with the ratio varying from 71.8% for γ_z ($\gamma_z^{-1/2}$) $=1.0$ (1.0) to 1.6% for γ_z ($\gamma_z^{-1/2}$)$=0.1$ (3.16). Energy levels become almost independent of the total spin as shown in Fig. 3(a). In addition, the system approaches the quasi-classical limit as $\gamma_z^{-1/2} \to \infty$. In Fig. 3(b), the shape of QD's varies from the oblate ellipsoid to the sphere and $E-\gamma_z$ is shown as a function of $\gamma_z^{-1/2}$. Similar to the prolate ones, splitting of degeneracy could be found if the shape varies from sphere to oblate ellipsoid. The states in which two electrons both oc-

TABLE I. Energy levels of two electrons in ellipsoidal QD's with two different shapes. For the sake of convenience, the short notation i.e., a, b, c, etc.—is used in all of the paper to indicate the quantum numbers $(n,m;N,M;s)$ and to show the change of the level order. The energy unit is Ry^*.

γ_{xy} ($\gamma_{xy}^{-1/2}$)	1.0 (1.0)		1.0 (1.0)	
γ_z/γ_{xy}	1		4	
a:(0, 0;0, 0;0)	(a)	4.0010	(a)	7.1805
b:(0, 0;0, 0;1)	(b)	4.7194	(c)	7.7889
c:(0, 1;0, 0;1)	(c)	4.7194	(e)	8.1805
d:(0, 1;0, 0;0)	(e)	5.0010	(f)	8.6254
e:(0, 0;0, 1;0)	(h)	5.0012	(g)	8.7889
f:(0, 2;0, 0;0)	(d)	5.5872	(h)	8.9541
g:(0, 1;0, 1;1)	(f)	5.5872	(i)	9.1805
h:(1, 0;0, 0;0)	(q)	5.5873	(o)	9.5324
i:(0, 0;1, 0;0)	(g)	5.7194	(j)	9.6254
j:(0, 2;0, 1;0)	(k)	5.7194	(k)	9.6968
k:(1, 1;0, 0;1)	(s)	5.7194	(l)	9.7889
l:(0, 1;1, 0;1)	(p)	5.7195	(m)	9.9541
m:(1, 0;0, 1;0)	(r)	5.8826	(n)	10.1804
n:(0, 0;1, 1;0)	(i)	6.0010	(q)	10.8181
o:(0, 3;0, 0;1)	(m)	6.0012	(b)	11.0008
p:(1, 0;0, 0;1)	(u)	6.5077	(r)	11.1805
q:(2, 0;0, 0;0)	(o)	6.5077	(d)	11.7270

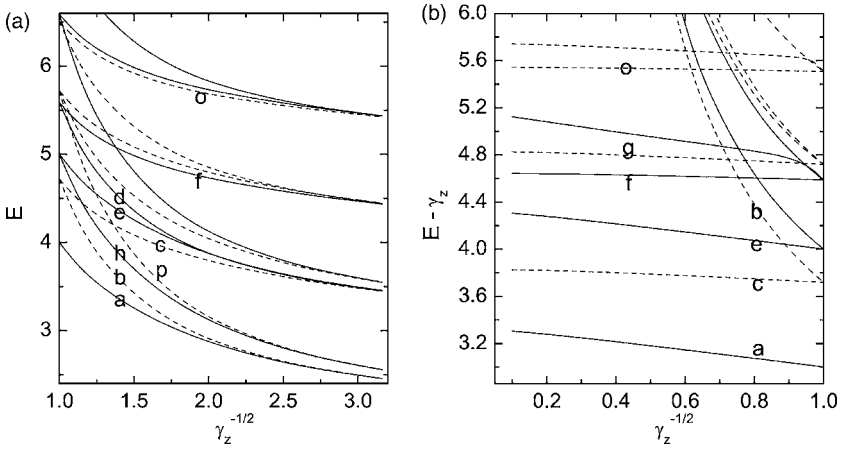

FIG. 3. Energy levels of spin-singlet (solid lines) and -triplet (dashed lines) states with $\gamma_{xy}=1.0$ as a function of $\gamma_z^{-1/2}$ in (a) prolate QD's and (b) oblate QD's where γ_z is subtracted in the total energy to clearly show the differences between the lower-energy levels.

cupy the z-directional ground state become the lowest-energy states in oblate QD's. The energy difference between states a and c becomes smaller in oblate QD's with respect to that in a spherical one.

Actually, Eq. (14) clearly shows the shape effect on the Coulomb energy. Particularly, we could obtain the Coulomb energy

$$E_{C,s}=\sqrt{\gamma}\frac{\Gamma(|m|+1)}{\Gamma\left(|m|+\frac{3}{2}\right)} \tag{15}$$

and

$$E_{C,2D}=\sqrt{\gamma}\frac{\Gamma\left(|m|+\frac{1}{2}\right)}{\Gamma(|m|+1)} \tag{16}$$

for spherical QD's with $\lambda=1$ and 2D QD's with $\lambda=\infty$, respectively. The ratio of $E_{C,2D}$ to $E_{C,s}$ is $\pi/2$ for $m=0$. In Fig. 4, we give the Coulomb energies of both prolate and oblate QD's as a function of $\gamma_z^{-1/2}$ and compare the perturbation results with the numerical ones. It can be seen that perturbation theory becomes ineffective in prolate QD's because of $E_C > \gamma_z$ in prolate QD's. The Coulomb energy of the state with $m=0$ decreases faster with respect to those of states with $m\neq 0$ as $\gamma_z^{-1/2}$ increases. The difference between Coulomb energies of two states with different m in the prolate QD's is much smaller than that in the oblate and spherical ones.

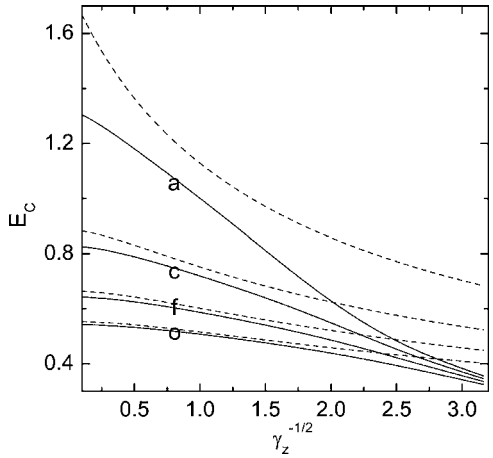

FIG. 4. Coulomb energies of ellipsoidal QD's with $\gamma_{xy}=1.0$ defined by Eq. (13) and obtained by the exact diagonalization (solid lines) and the perturbation calculation (dashed lines) as a function of $\gamma_z^{-1/2}$.

B. Shape and size effects on the spin transition

The spin transition of the ground state under magnetic field is one of the most interesting phenomena in QD's,[26,27] and it has been theoretically investigated for potential applications in quantum information in which the spin is used as a qubit.[23,24] Here we have investigated the spin transition and the corresponding shape and size effects in ellipsoidal QD's whose geometric configuration is close to that of the realistic QD's.

We have performed numerical calculations on spectra of two electrons in QD's in magnetic field. The energy levels normalized by γ_{xy} are shown as a function of γ_B in Figs. 5(a) and 5(b) for a spherical QD and a prolate QD, respectively. We note that there is a crossing between triplet states b and $c-$ in the prolate QD, unlike the spherical one. There are spin transitions of the ground states in both spherical and prolate QD's; however, the spin transition in the prolate QD needs a stronger magnetic field.

In order to better understand the spin transition of ground states, we use Eq. (14) to obtain the energy difference ΔE between the lowest triplet state E_t and the lowest singlet one E_s in a strong magnetic field. Generally, we can obtain the ΔE between the two lowest states $(0,-2k-1,0,0,1)$ and $(0,-2l,0,0,0)$ as follows:

$$\Delta E=\Delta E_0+\Delta E_C, \tag{17}$$

with

$$\Delta E_0=\gamma_{xy}(2k-2l+1)\left[\sqrt{1+\left(\frac{\lambda_B}{2}\right)^2}-\frac{\lambda_B}{2}\right] \tag{18}$$

and

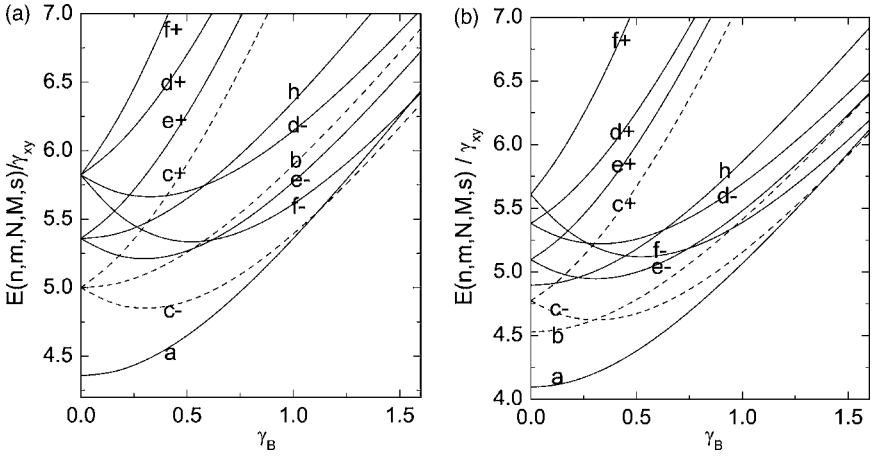

FIG. 5. Energy levels of spin-singlet (solid lines) and -triplet (dashed lines) states normalized by γ_{xy} as a function of γ_B in (a) a spherical QD with $\gamma_{xy}=\gamma_z=0.5$ and (b) a prolate QD with $\gamma_{xy}=0.5$, $\gamma_z=0.4$. $c-$, $e-$, $f-$, and $d-$ ($c+$, $e+$, $f+$, and $d+$) represent the corresponding states with negative (positive) azimuthal quantum numbers.

$$\Delta E_C = \sqrt{\lambda_0 \gamma_{xy}} \left[\frac{\Gamma(2k+2)}{\Gamma\left(2k+\frac{5}{2}\right)} F\left(\frac{1}{2}, 2k+2; 2k+\frac{5}{2}; 1-\lambda\right) - \frac{\Gamma(2l+1)}{\Gamma\left(2l+\frac{3}{2}\right)} F\left(\frac{1}{2}, 2l+1; 2l+\frac{3}{2}; 1-\lambda\right) \right], \quad (19)$$

where ΔE_C is the Coulomb energy difference between the corresponding two states, $\lambda=\lambda_0/\sqrt{1+(\lambda_B/2)^2}$, with $\lambda_0=\gamma_z/\gamma_{xy}$ and $\lambda_B=\gamma_B/\gamma_{xy}$, and $k,l=0,1,2,\ldots$. As λ_B increases, $k-l$ is 0 for the singlet to the triplet transition and -1 for the triplet to the singlet transition. When $k-l=0$, ΔE_0 is positive and ΔE_C is negative, while it is reverse for $k-l=-1$. Just because of the opposite signs between ΔE_0 and ΔE_C, ΔE could be zero. It means that both the magnetic field and the Coulomb interaction induce the spin transition in QD's. ΔE of Eq. (17) is not only influenced by the size (γ_{xy}), but also by the shape (λ_0).

We plot the ΔE as a function of λ_B for various λ_0 in Figs. 6(a) and 6(b) with $\gamma_{xy}=2.0$ and 0.5, respectively. It shows that the perturbation theory gives the qualitative picture of the spin transition and is more effective for larger γ_{xy}. However, numerical calculation is necessary to obtain an accurate spin phase diagram. It is obvious that the spin transition occurs at a larger magnetic field in the prolate QD's since the absolute value of ΔE_C in the prolate QD's is much less than that of the oblate ones, which can be seen in Fig. 4. Therefore, it can be concluded that magnetic field could more easily induce the spin transition in weakly confined oblate QD's. This is consistent with results of Ref. 24, in which the spin transition of vertically coupled QD's could be influenced by the in-plane magnetic field which changes effective shape of QD's.

IV. SUMMARY

In conclusion, a computational method is introduced for two-electron spectra in ellipsoidal QD's, in which matrix elements can be analytically obtained. The perturbation formulas are also analytically given. The calculated results of spherical QD's obtained by the method are in good agreement with exact ones. Two-electron spectra and Coulomb interaction energies in both prolate and oblate QD's are compared. There are obvious size and shape effects on the energy levels and their orders. The effects are attributed to the competition between confinement and interaction energies. The spin transition induced by a magnetic field is strongly influenced by the size and shape, and it occurs at a larger magnetic field in prolate QD's, which is consistent with Ref. 24. It is important to point out that the two-electron levels are almost independent of the total spin as the value of $\gamma_z^{-1/2}$ is

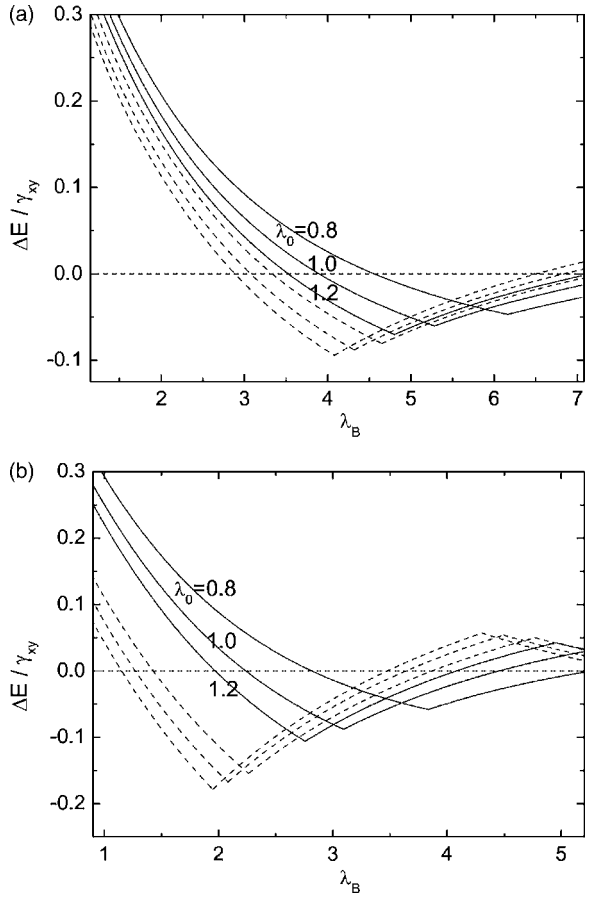

FIG. 6. ΔE obtained by the exact diagonalization (solid lines) and the perturbation calculation (dashed lines) and normalized by γ_{xy} as a function of λ_B for $\lambda_0=0.8$, 1.0, and 1.2 with (a) $\gamma_{xy}=2.0$ and (b) $\gamma_{xy}=0.5$.

much larger than that of $\gamma_{xy}^{-1/2}$. The reasons are clearly given by both the exact diagonalization and the perturbation calculation. What are mentioned above are useful to investigate and understand the electronic and magnetic properties of various 3D QD's. Furthermore, the calculation method can be applied to vertically coupled QD's, which may be used as a quantum gate, and work is in progress.

ACKNOWLEDGMENTS

Financial support from NSF-China (Grant No. 10374057) and China's "863" Programme is gratefully acknowledged.

APPENDIX

The Coulomb interaction matrix elements V can be analytically obtained as follows:

$$\begin{aligned} &V(i_1,i_2,m,j_1,k_1,j_2,k_2,A) \\ &= \left\langle \Phi^r_{i_1,m}\Theta_{j_1,k_1,A} \left| \frac{2}{\sqrt{r^2+(z_1-z_2)^2}} \right| \Phi^r_{i_2,m}\Theta_{j_2,k_2,A} \right\rangle \\ &= \sum_{l=2|m|}^{2(i_1+i_2+|m|)} \sum_{n_1=0}^{k_1+k_2} \sum_{n_2=0}^{k_1+k_2} C^{i_1,i_2,m,j_1,k_1,j_2,k_2,A}_{l,n_1,n_2} \\ &\quad \times I_{l,n_1,n_2}(r,z_1,z_2), \end{aligned} \tag{A1}$$

with

$$\begin{aligned} I_{l,n_1,n_2}(r,z_1,z_2) &= \int_0^\infty \mathrm{d}r \int_{-\infty}^\infty \mathrm{d}z_1 \int_{-\infty}^\infty \mathrm{d}z_2 r^l z_1^{n_1} z_2^{n_2} \\ &\quad \times \frac{e^{-\beta r^2} e^{-\alpha z_1^2} e^{-\alpha z_2^2}}{\sqrt{r^2+(z_1-z_2)^2}}, \end{aligned} \tag{A2}$$

where $\beta=\gamma/4$, $\alpha=\gamma_z/2$, and $C^{i_1,i_2,m,j_1,k_1,j_2,k_2,A}_{l,n_1,n_2}$ is the expansion coefficient. Taking

$$a = \frac{z_1-z_2}{\sqrt{2}}, \quad b = \frac{z_1+z_2}{\sqrt{2}}, \tag{A3}$$

we substitute Eq. (A3) into Eq. (A2) and then

$$\begin{aligned} I_{l,n_1,n_2} &= \int_0^\infty \mathrm{d}r \int_{-\infty}^\infty \mathrm{d}a \int_{-\infty}^\infty \mathrm{d}b \frac{r^l e^{-\beta r^2} e^{-\alpha a^2} e^{-\alpha b^2}}{\sqrt{r^2+(\sqrt{2}a)^2}} \\ &\quad \times \frac{(a+b)^{n_1}(b-a)^{n_2}}{\sqrt{2}^{n_1+n_2}} \\ &= \sum_{i=0}^{n_1} \sum_{j=0}^{n_2} C^i_{n_1} C^j_{n_2} \sqrt{2}^{-n_1-n_2} \int_0^\infty \mathrm{d}r \int_{-\infty}^\infty \mathrm{d}a \int_{-\infty}^\infty \mathrm{d}b \\ &\quad \times \frac{r^l e^{-\beta r^2} e^{-\alpha a^2} e^{-\alpha b^2}}{\sqrt{r^2+(\sqrt{2}a)^2}} b^{i+j} a^{n_1+n_2-i-j} (-1)^{n_2-j}. \end{aligned} \tag{A4}$$

Integration of b is separated analytically. Now we deal with the integration on a and r in the following form:

$$\int_0^\infty \mathrm{d}r \int_{-\infty}^\infty \mathrm{d}a \frac{r^l e^{-\beta r^2} e^{-\alpha a^2}}{\sqrt{r^2+(\sqrt{2}a)^2}} a^k, \tag{A5}$$

in which k is the non-negative integers. Defining $p=\sqrt{\alpha}a$, $q=\sqrt{\beta}r$, we substitute them into Eq. (A5):

$$\int_0^\infty \mathrm{d}q \int_{-\infty}^\infty \mathrm{d}p \frac{q^l e^{-q^2} e^{-p^2}}{\sqrt{p^2+\mu q^2}} p^k \frac{1}{\sqrt{2}\sqrt{\alpha}^k \sqrt{\beta}^{l+1}}, \tag{A6}$$

in which $\mu=\alpha/2\beta=\gamma_z/\gamma$. Defining $q=\tau\cos\theta$, $p=\tau\sin\theta$, we substitute them into Eq. (A6) and then

$$\begin{aligned} &\int_0^\infty \mathrm{d}\tau \int_{-\pi/2}^{\pi/2} \mathrm{d}\theta \frac{\tau e^{-\tau^2}}{\sqrt{(\tau\sin\theta)^2+\mu(\tau\cos\theta)^2}} \\ &\quad \times (\tau\cos\theta)^l (\tau\sin\theta)^k \frac{1}{\sqrt{2}\sqrt{\alpha}^k\sqrt{\beta}^{l+1}} \\ &= \int_0^\infty \mathrm{d}\tau \int_{-\pi/2}^{\pi/2} \mathrm{d}\theta \frac{e^{-\tau^2}}{\sqrt{(\sin\theta)^2+\mu(\cos\theta)^2}} \\ &\quad \times (\cos\theta)^l (\sin\theta)^k \tau^{l+k} \frac{1}{\sqrt{2}\sqrt{\alpha}^k\sqrt{\beta}^{l+1}} \\ &= \int_{-\pi/2}^{\pi/2} \mathrm{d}\theta (\cos\theta)^l (\sin\theta)^k \frac{1}{\sqrt{(\sin\theta)^2+\mu(\cos\theta)^2}} \\ &\quad \times \frac{\Gamma\left(\frac{1+l+k}{2}\right)}{2\sqrt{2}\sqrt{\alpha}^k\sqrt{\beta}^{l+1}}. \end{aligned} \tag{A7}$$

It is easy to find that the integration on θ is nonzero if and only if k is an even integer—i.e., $k=2u$, where u is an integer:

$$\begin{aligned} &\int_{-\pi/2}^{\pi/2} \mathrm{d}\theta (\cos\theta)^l (\sin\theta)^k \frac{1}{\sqrt{(\sin\theta)^2+\mu(\cos\theta)^2}} \\ &= \frac{\Gamma\left(\frac{1+l}{2}\right)\Gamma\left(\frac{1}{2}+u\right)}{\Gamma\left(1+\frac{l}{2}+u\right)} F\left(\frac{1}{2},\frac{1+l}{2};1+\frac{l}{2}+u;1-\mu\right). \end{aligned} \tag{A8}$$

*Electronic address: zjl-dmp@mail.tsinghua.edu.cn

[1] L. P. Kouwenhoven, T. H. Oosterkamp, M. W. S. Danoesastro, M. Eto, D. G. Austing, T. Honda, and S. Tarucha, Science **278**, 1788 (1997).

[2] T. H. Oosterkamp, T. Fujisawa, W. G. van der Wiel, K. Ishibashi, R. V. Hijman, S. Tarucha, and L. P. Kouwenhoven, Nature (London) **395**, 873 (1998).

[3] N. F. Johnson, J. Phys.: Condens. Matter **7**, 965 (1995).

[4] D. G. Austing, S. Sasaki, S. Tarucha, S. M. Reimann, M. Koskinen, and M. Manninen, Phys. Rev. B **60**, 11514 (1999).
[5] L. L. Sun, F. C. Ma and S. S. Li, J. Appl. Phys. **94**, 5844 (2003).
[6] P. S. Drouvelis, P. Schmelcher, and F. K. Diakonos, Phys. Rev. B **69**, 155312 (2004).
[7] X. Z. Liao, J. Zou, X. F. Duan, D. J. H. Cockayne, R. Leon, and C. Lobo, Phys. Rev. B **58**, R4235 (1998).
[8] X. Z. Liao, J. Zou, D. J. H. Cockayne, R. Leon, and C. Lobo, Phys. Rev. Lett. **82**, 5148 (1999).
[9] M. Bayer, P. Hawrylak, K. Hinzer, S. Fafard, M. Korkusinski, Z. R. Wasilewski, O. Stern, and A. Forchel, Science **291**, 451 (2001).
[10] B. Meurer, D. Heitmann, and K. Ploog, Phys. Rev. B **48**, 11488 (1993).
[11] X. G. Peng, L. Manna, W. D. Yang, J. Wickham, E. Scher, A. Kadavanich, and A. P. Alivisatos, Nature (London) **404**, 59 (2000).
[12] M. Shim and P. Guyot-Sionnest, Nature (London) **407**, 981 (2000).
[13] S. H. Kan, T. Mokari, E. Rothenberg, and U. Banin, Nat. Mater. **2**, 155 (2003).
[14] J. T. Hu, L. S. Li, W. D. Yang, L. Manna, L. W. Wang, and A. P. Alivisatos, Science **292**, 2060 (2001).
[15] X. Chen, A. Nazzal, D. Goorskey, M. Xiao, Z. A. Peng, and X. G. Peng, Phys. Rev. B **64**, 245304 (2001).
[16] H. Htoon, J. A. Hollingworth, A. V. Malko, R. Dickerson, and V. I. Klimov, Appl. Phys. Lett. **82**, 4776 (2003).
[17] M. B. Mohamed, C. Burda, and M. A. El-Sayed, Nano Lett. **1**, 589 (2001).
[18] G. Cantele, D. Ninno, and G. Iadonisi, J. Phys.: Condens. Matter **12**, 9019 (2000).
[19] G. Cantele, G. Piacente, D. Ninno, and G. Iadonisi, Phys. Rev. B **66**, 113308 (2002).
[20] X. Z. Li and J. B. Xia, Phys. Rev. B **66**, 115316 (2002).
[21] L. C. Lew Yan Voon, R. Melnik, B. Lassen, and M. Willatzen, Nano Lett. **4**, 289 (2004).
[22] G. Cantele, D. Ninno, and G. Iadonisi, Phys. Rev. B **64**, 125325 (2001).
[23] G. Burkard, G. Seelig, and D. Loss, Phys. Rev. B **62**, 2581 (2000).
[24] D. Bellucci, M. Rontani, F. Troiani, G. Goldoni, and E. Molinari, Phys. Rev. B **69**, 201308(R) (2004).
[25] J. L. Zhu, Z. Q. Li, J. Z. Yu, K. Ohno, and Y. Kawazoe, Phys. Rev. B **55**, 15819 (1997).
[26] J. L. Zhu, Z. Zhu, Y. Kawazoe, and T. Yao, Phys. Rev. B **58**, 13755 (1998).
[27] M. Dineykhan and R. G. Nazmitdinov, Phys. Rev. B **55**, 13707 (1997).